Prospects for radio detection of extensive air showers in the atmosphere of Jupiter

DOI:
10.3847/0004-637X/825/2/129

Document Version
Accepted author manuscript

Prospects for radio detection of extensive air showers in the atmosphere of Jupiter

J. D. Bray
JBCA, School of Physics & Astronomy, University of Manchester, Manchester M13 9PL, UK
justin.bray@manchester.ac.uk

A. Nelles
Department of Physics & Astronomy, University of California, Irvine, CA 92697, USA

ABSTRACT

Rimmer et al. (2014) recently suggested that it may be possible to detect radio emission from extensive air showers produced by ultra-high-energy cosmic rays interacting in the atmosphere of Jupiter, effectively using Jupiter as a cosmic-ray detector. We investigate the potential of this approach and find that, although the effective detector area ($\sim 2.5 \times 10^7$ km^2) is substantial, the acceptance angle is so small that the typical geometric aperture ($\sim 10^3$ km^2 sr) is less than that of existing terrestrial detectors. Furthermore, we find that the sensitivity of current or planned radio telescopes is insufficient to detect cosmic rays below a threshold energy of $\sim 10^{23}$ eV. Exploitation of the large surface area of Jupiter for detecting cosmic rays remains a long-term prospect that will require a different technique, such as orbital fluorescence detection.

Subject headings: astroparticle physics — cosmic rays — planets and satellites: individual (Jupiter)

1. Introduction

The spectrum of ultra-high-energy cosmic rays decreases steeply at energies above 10^{20} eV (Abraham et al. 2010). Detecting the rare particles at higher energies requires detectors with extremely large apertures, which may potentially be obtained through remote monitoring of planet-sized bodies (Gorham 2004) such as Earth (e.g. Takahashi 2009) or the Moon (e.g. Bray et al. 2015a). As the largest body available in the solar system — apart from the Sun — Jupiter is an attractive option for this approach. Rimmer et al. (2014) recently suggested that cosmic rays interacting in the atmosphere of Jupiter could be detected from their gamma-ray or radio emission, and that this was practical with present-day instruments.

Privitera & Motloch (2014) argue that the result of Rimmer et al. is incorrect. When a cosmic ray interacts in an atmosphere, a shower of particles develops, generating and entraining additional particles until the energy per particle drops low enough that ionization losses dominate, and the shower dissipates. Privitera & Motloch calculate the aperture viewed by an orbiting satellite, requiring that the paths of detectable cosmic rays must pass through a column density of at least 600 g/cm^2, so a shower can develop a detectable number of gamma rays, but no more than 1200 g/cm^2, so the shower is not completely attenuated; these values are typical for a shower in the terrestrial atmosphere. They find apertures for Earth and other solar system objects that are lower than those of existing detectors. For Jupiter, they additionally find that the resulting gamma rays are insufficiently intense to be detected at the distance of Earth.

The rebuttal of Privitera & Motloch does not, however, apply to radio emission from a shower: radio waves are much less attenuated by an atmosphere than are gamma rays, so cosmic rays can be observed through much greater atmospheric

column densities. Their analysis of the intensity of the emission also applies only to gamma rays, as the radio emission will have a different intensity, and gamma-ray and radio telescopes are not equally sensitive.

In this work we perform a more detailed analysis of the development (Section 2) and radio emission (Section 3) of a Jovian air shower. In Section 4 we examine the interaction geometry and the consequent geometric aperture, and in Section 5 we consider the prospects for detecting the radio emission with a realistic experiment. We discuss in Section 6 the implications of our results for the potential of Jupiter as a cosmic-ray detector.

2. Development of Jovian air showers

The environment on Jupiter differs from Earth in several ways which will affect the development of an extensive air shower.

- The atmosphere of Jupiter is 75% molecular hydrogen by mass, with the remainder composed almost entirely of helium. Several characteristic quantities are therefore quite different, as shown in Table 1; in particular, the radiation length is almost doubled.
- Due to the greater scale height of the Jovian atmosphere, a shower penetrating down through a given column density will develop in a less dense medium, as for inclined showers on Earth. As we shall see in Section 4, the geometry for a detectable Jovian air shower requires that it be highly inclined, exacerbating this effect.
- The magnetic field of Jupiter is stronger than that of Earth, with a strength of 400 μT at the equator and 1100–1400 μT at the poles (Smith et al. 1974), versus equivalent values of 35 μT and 65 μT respectively for the geomagnetic field (Finlay et al. 2010).

To determine the effect of this differing environment on the development of an air shower, we carry out a series of simulations with the AIRES code (Sciutto 1999). AIRES has been developed to simulate showers in a terrestrial atmosphere, so to represent the Jovian atmosphere we use the TIERRAS extension (Tueros & Sciutto 2010), which allows for simulations in other media such as ice or soil. Using this extension we define a custom Jovian atmosphere, using the values for a hydrogen-helium mixture from Table 1 (except for the density, which we vary between simulations). For simplicity, in all simulations we take the primary cosmic ray to be a proton. At higher energies it is arguable that this should be a heavier nucleus (Aab et al. 2014), but this will have only a minor effect on the dominant electromagnetic component of the shower and on the resulting radio emission (Nelles et al. 2015).

The longitudinal development profiles of some simulated showers are shown in Figure 1, isolating the effects of each of the environmental differences listed above. The composition of the Jovian atmosphere causes the electromagnetic cascade to be elongated compared to a terrestrial shower, the reduced density suppresses the muon flux by allowing more decays, and the Jovian magnetic field, using a representative strength of 800 μT, causes the electromagnetic cascade to be strongly suppressed, as the high-energy electrons and positrons rapidly lose energy to synchrotron radiation. The synchrotron photons in this regime are high-energy gamma rays which continue to participate in the shower, but this loss still causes the shower to initially develop and attenuate more rapidly than when electrons and positrons produce gamma rays primarily through bremsstrahlung as in a classical electromagnetic cascade. This last effect, in particular, reduces the peak number of charged particles by a factor ~ 4, significantly decreasing the potential for detecting the radio emission of a Jovian air shower. The first effect also suggests a modification to the calculations of Privitera & Motloch (2014) for the case of Jupiter, as the shower maximum occurs at a column density of $X_{\max} \sim 1500$ g/cm^2 rather than in their assumed range of 600–1200 g/cm^2, but this is unlikely to make a large difference to their result.

3. Radio emission from Jovian air showers

When an extensive air shower develops in the atmosphere of Jupiter, as on Earth, the positively and negatively charged particles in the shower (primarily electrons and positrons) are deflected in opposite directions by the Jovian magnetic field. As electrons and positrons are continuously produced and deflected over the life of the shower,

Table 1
Standard parameters for Jovian and terrestrial atmospheric gases

Composition (by mass)	Density[a] (g/cm^3)	Refractive index[a]	Radiation length (g/cm^2)	Effective Z	Mean Z/A
100% H_2	0.000071	1.000132	63.04	1	0.9921
100% He	0.000125	1.000035	94.32	2	0.4997
75% H_2/25% He[b]	0.000085	1.000118	68.74	1.257[c]	0.8690
terrestrial air	0.001205	1.000289	37.10	7.265[c]	0.4992

[a]At standard temperature and pressure.

[b]Representative of the Jovian atmosphere.

[c]Calculated per method II of Henriksen & Baarli (1957).

References. — (Olive et al. 2014; Sciutto 1999)

they give rise to a time-varying transverse current which is responsible for the majority of the shower radio emission. The basic principles of this emission have been understood for some time (Kahn & Lerche 1966; Allan 1971), and modern microscopic simulations produce results that closely match radio observations of terrestrial air showers; see Huege (2016) for a review.

Rimmer et al. (2014) develop their own model in which they represent the radio emission from a shower as classical synchrotron radiation. This implicitly assumes that charged particles in the shower follow collisionless, circular paths, which has proven to be a poor approximation to real air showers (Huege 2016, Section 3.1). Rimmer et al. also assume perfect coherence between charged particles in the shower, with the resulting emission spectrum peaking at a frequency of 50 GHz, whereas the spectra of air showers are dominated by decoherence effects, with strong, coherent radiation being emitted only at substantially lower frequencies.

In this work, rather than developing our own model, we extend our simulations from Section 2 by calculating the radio emission with the ZHAireS code (Alvarez-Muñiz et al. 2012), which has been validated against observations of terrestrial air showers (Buitink et al. 2016). An additional parameter required by this code is the refractive index of the Jovian atmosphere, which we take to be

$$n_\mathrm{r} = 1 + 0.000140 \times \left(\frac{\rho}{10^{-4}\ \mathrm{g\,cm^{-3}}} \right) \quad (1)$$

in terms of the density ρ, for non-standard temperature and pressure, based on the values in Table 1.

For an observer at the Cherenkov angle

$$\theta_\mathrm{c} = \arccos(1/n_\mathrm{r}) \quad (2)$$

from the shower axis, the entire shower is observed near-simultaneously. Coherency over the length of the shower, and hence the amplitude of the emitted radio pulse, are therefore maximised when the observer is within a small angle $\Delta\theta$ from the Cherenkov angle. Sample pulses are shown in Figure 2, illustrating this.

To find the spectra of these pulses over frequency ν, we take their complex Fourier transform, convolve this with a variable-width window of fractional bandwidth $\Delta\nu/\nu = 0.5$, and take the magnitude of the result. This represents an observation with a corresponding experimental bandwidth, but the effect of varying this assumption is minor: for practical purposes, this is just a smoothing operation. The resulting spectra are shown in Figure 3. Depending on $\Delta\theta$, the spectra generally cut off at frequencies below a few GHz, so detection at 50 GHz as suggested by Rimmer

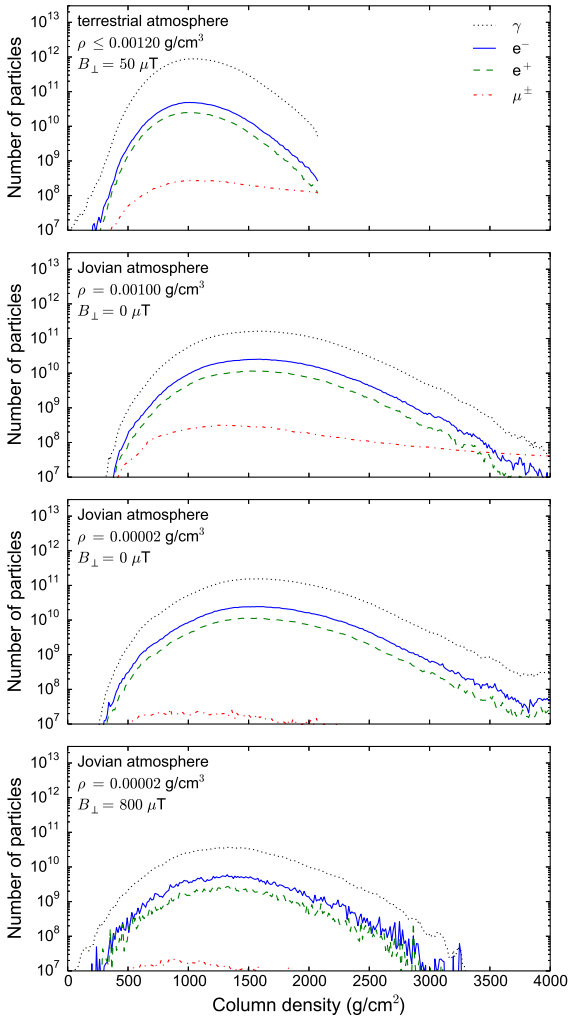

Fig. 1.— Longitudinal development of simulated air showers in terrestrial and Jovian conditions, showing the dominant particle species. The primary cosmic ray in each case is a proton with an energy of 10^{20} eV. Compared to the terrestrial air shower (top), a shower in the Jovian atmosphere with comparable density ρ (upper center) develops at a greater column density because of the increased radiation length of this medium. In the less-dense upper atmosphere of Jupiter (lower center), where a detectable air shower is more likely to develop (see Section 4), muons are less numerous, because the larger physical distance associated with a given column density makes them more likely to decay. The introduction of the Jovian magnetic field with a realistic transverse field strength $B_\perp$ (bottom) causes the shower to be strongly suppressed by synchrotron losses.

et al. is unlikely. Observations at low frequencies are limited, however, by the background Jovian decametric radiation, with an intensity of $\sim 10^6$ Jy (Warwick 1967). This radiation cuts off sharply at a frequency of 40 MHz, corresponding to the maximum cyclotron frequency in the local magnetic field, so this may be taken as a lower limit to the frequency for practical detection of Jovian air showers.

The beam pattern of the emission around the Cherenkov angle, and the dependence on the energy E of the shower and the density of the medium, are shown in Figure 4. Taking a frequency-dependent Gaussian beam shape per Alvarez-Muñiz et al. (2006), and assuming a linear dependence on shower energy and a power-law dependence on density, we apply a rough parametrisation of the spectral electric field as

$$\mathcal{E}(\nu,\theta;E,\rho,l) = \mathcal{E}_0 \left(\frac{E}{10^{20}\text{ eV}}\right)\left(\frac{\rho}{0.00001\text{ g/cm}^3}\right)^{\alpha} \times \left(\frac{l}{8\times10^{11}\text{ m}}\right)^{-1} \exp\left(-\left(\frac{\Delta\theta}{\theta_c}\right)^2\left(\frac{\nu}{\nu_0}\right)^2\right) \quad (3)$$

where $l = 8 \times 10^{11}$ m is the mean distance from Earth to Jupiter. For the free parameters in this expression we fit the values

$$\mathcal{E}_0 = 5.7\times10^{-7}\ \mu\text{V/m/MHz} \quad (4)$$
$$\nu_0 = 6.9\text{ MHz} \quad (5)$$
$$\alpha = 0.94 \quad (6)$$

using a series of simulations spanning the ranges 10^{19}–10^{21} eV in energy and 0.00001–0.00005 g/cm^3 in density. Testing these values against another simulation, we find them to give results accurate to within a factor of two in $\Delta\theta$ in this parameter range. We expect the linear dependence on E to hold reasonably well outside this range, as this linearity is a consistent feature of coherent pulses from particle cascades.

4. Calculation of geometric aperture

For a cosmic ray interacting in the Jovian atmosphere to be detected, it must meet two conditions: the interaction must be sufficiently deep that the extensive air shower will fully develop and produce coherent radio emission, and sufficiently shallow that this radio emission — directed forward along

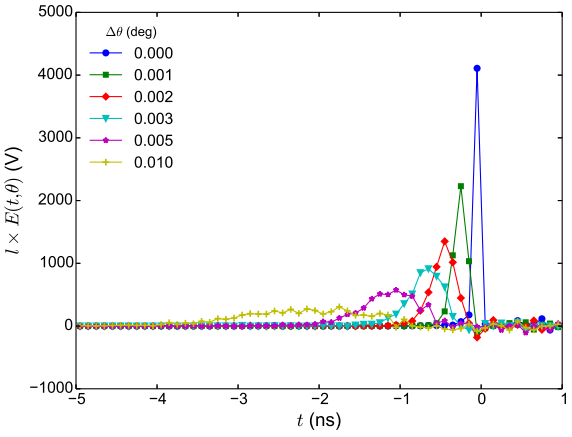

Fig. 2.— Radio pulses from a simulated Jovian air shower, showing electric field strength $E(t, \theta)$ at distance l in the far field. At greater angles $\Delta\theta$ inside the Cherenkov cone, the pulse is broader and weaker; angles outside the Cherenkov cone (not shown) display the same effect. The shower shown here had a primary cosmic-ray proton with an energy of 10^{20} eV, and developed in a Jovian atmosphere with a density of 0.00002 g/cm^{-3}.

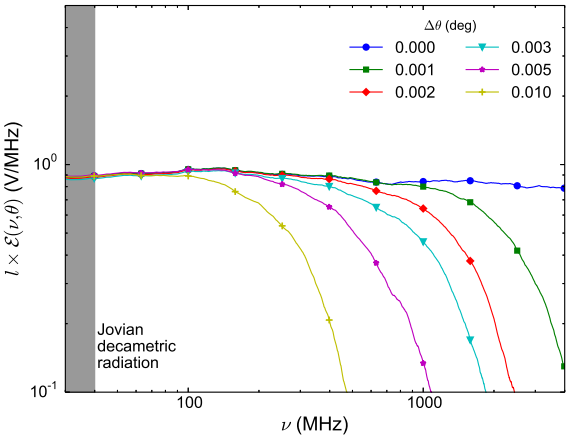

Fig. 3.— Spectra of the simulated radio pulses shown in Figure 2, showing spectral electric field strength $\mathcal{E}(\nu, \theta)$, smoothed as described in the text. At greater angles $\Delta\theta$ inside the Cherenkov cone, the pulse loses coherence and becomes weaker at higher frequencies. The shaded region shows the frequency range in which detection of the pulse is impractical because of the background Jovian decametric radiation.

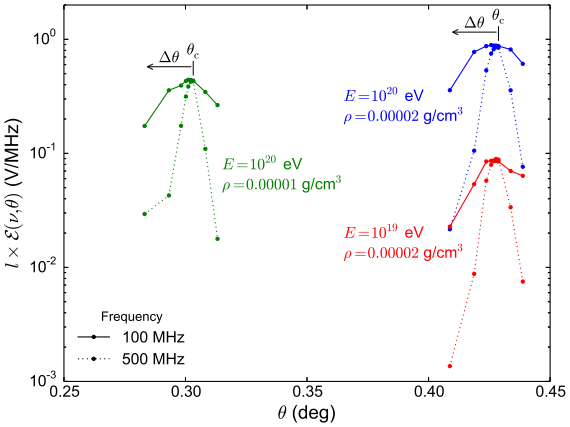

Fig. 4.— Beam patterns of radio pulses from simulated Jovian air showers, showing spectral electric field strength $\mathcal{E}(\nu, \theta)$ at distance l in the far field. The radiation is beamed as a hollow cone at the Cherenkov angle $\theta = \theta_c$ from the axis of the shower. If the shower develops at a lower atmospheric density (left; green), then the emission is weaker than for a similar shower at a higher density (top-right; blue), and the Cherenkov angle is smaller. If the shower has a lower energy (bottom-right; red), the emission is weaker but the Cherenkov angle is unchanged. In all cases, the radiation has a smaller beam width scale $\Delta\theta$ at higher frequencies.

the axis of the shower — is not completely attenuated as it escapes the atmosphere. These conditions constrain detectable cosmic rays to trajectories that skim the atmosphere of Jupiter, as described by Rimmer et al. (2014) and illustrated in Figure 5. The detection region is an annulus around Jupiter with a width of ΔR and a circumference of $2\pi R_{\rm J}$, where $R_{\rm J} = 6.9 \times 10^4$ km is the mean radius of Jupiter.

For the full development of an air shower, we require that it reach a column depth of $X_{\rm max} \sim 1500$ g/cm^{-2}, corresponding to the depth of maximum development in the lower panel of Figure 1, before the lowest-altitude point on its path. This point must therefore be deep enough that the total column density $X_{\rm tot}$ along its path, which we calculate from the atmospheric density profile of Moses et al. (2005), exceeds 3000 g/cm^2. For the radio emission to escape, we require that the projected shower axis pass no deeper than a pressure of 1000 mbar, at which Lindal et al. (1981) found the S-band signal from the Voyager 1 probe at 2.3 GHz to be extinguished due to absorption by ammonia. Between these two altitudes we find a range of $\Delta R = 57$ km as shown in Figure 6. The lower altitude in particular is only an approximate limit, as it most likely corresponds to several optical depths of radio attenuation, and also varies with frequency. However, due to the exponential profile of the atmosphere, refining these assumptions will have a relatively small effect on ΔR.

The resulting area of the annular detection region is $2\pi R_{\rm J} \Delta R = 2.5 \times 10^7$ km^2, which is substantial: it exceeds the area of the Pierre Auger Observatory (Aab et al. 2015), the largest current cosmic-ray detector, by four orders of magnitude. However, a cosmic ray passing through this area will only be detected if its beamed emission is directed towards a radio antenna. The resulting acceptance angle for a detectable cosmic ray, assuming a single radio antenna (e.g. at Earth), has the same solid angle as the emission, or

$$\Omega = 4\pi\, \theta_{\rm c}\, \Delta\theta_{\rm max} \qquad (7)$$

where $\Delta\theta_{\rm max}$ is the maximum separation from the Cherenkov angle at which the pulse can be detected. For a typical Cherenkov angle and beam scale width of $\theta_{\rm c} \sim 0.4°$ and $\Delta\theta_{\rm max} \sim 0.02°$ respectively (see Figure 4), this results in a geomet-

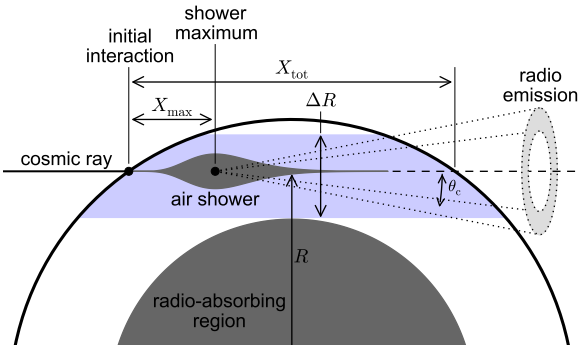

Fig. 5.— Interaction geometry for a detectable Jovian air shower. The shower develops from the initial interaction, reaching its maximum development at a column depth $X_{\rm max} \sim 1500$ g/cm^2. The radio emission from the shower is beamed forward as a hollow cone at the Cherenkov angle $\theta_{\rm c}$ around the projected shower axis (dashed). For the shower to be detectable, it must be sufficiently deep that the total column density $X_{\rm tot}$ allows it to completely develop, but not so deep that the radio emission is absorbed.

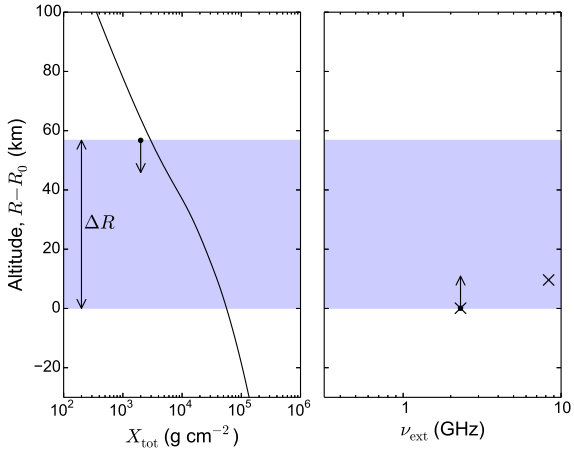

Fig. 6.— Range of altitudes (shaded) for the lowest point on the projected path of a detectable cosmic ray through the Jovian atmosphere, at radius R as illustrated in Figure 5. We require that the column density $X_{\rm tot}$ along the path of the cosmic ray be at least 3000 g/cm^2 (left), and that the path pass no deeper than the altitude at which the signal from Voyager 1 was extinguished at a frequency $\nu_{\rm ext} = 2.3$ GHz (right). The reference zero altitude, at radius R_0, is at a pressure of 1000 mbar.

ric aperture of $2\pi R_{\rm J}\Delta R\,\Omega \sim 10^3$ km^2 sr, which is less than current detectors.

More generally, we can find the geometric aperture as

$$A(E;\mathcal{E}_{\rm thr}) = \int_{R_{\rm min}}^{R_{\rm max}} 2\pi R_{\rm J}\, dR\ \Omega(\mathcal{E}_{\rm thr}) \qquad (8)$$

where $\Omega(\mathcal{E}_{\rm thr})$ is the solid angle in which the pulse amplitude exceeds a detection threshold of $\mathcal{E}_{\rm thr}$. To calculate this value, we first solve Equation 3 for $\Delta\theta$ with $\mathcal{E} = \mathcal{E}_{\rm thr}$, and then use this value as $\Delta\theta_{\rm max}$ when calculating Ω from Equation 7. We assume in Equation 3 that ρ is evaluated at a column depth of $X_{\rm max} = 1500$ g/cm^2 along the shower axis, effectively assuming that the entire cascade occurs in a medium corresponding to the density at the shower maximum. Across the altitude range ΔR, these densities take values 0.000012–0.000036 g/cm^3, falling within the parameter range of our simulations in Section 3. Some sample apertures for idealised Earth-based radio antennas are shown in Figure 7. In the following section, we consider the prospects of detecting cosmic rays with some realistic experiments.

5. Detection prospects

To date, the experiment with the greatest sensitivity to coherent astronomical pulses is the LUNASKA Parkes experiment (Bray et al. 2015a), which used the Parkes radio telescope to search for pulses from particle cascades in the lunar regolith. The most sensitive future radio telescope currently being developed, Phase 1 of the Square Kilometre Array, will have substantially greater sensitivity in the same role (Bray et al. 2015b). If these telescopes were used instead to search for radio pulses from Jupiter, they would constitute experiments capable in principle of detecting Jovian air showers, albeit with some technical challenges such as compensating for dispersion of the pulse in the Jovian ionosphere. Parameters for these experiments are listed in Table 2.

Another possibility is to search for radio pulses using an antenna on a Jupiter-orbiting satellite, which has the advantage of closer proximity to the source of the pulse. The Juno probe, arriving at Jupiter in July 2016, is equipped with a microwave radiometer (MWR; Janssen et al. 2014; Janssen 2015) which we shall use as an example of such an instrument. The lowest-frequency antenna of this instrument operates at 600 MHz with a bandwidth of 21 MHz and a beam width of 20°, which implies an antenna area of ~ 2 m^2. Assuming the system temperature to be dominated by the ~ 700 K brightness temperature of Jupiter at this frequency, the noise level can then be calculated as $\mathcal{E}_{\rm rms} = 0.29$ μV/m/MHz (Bray 2016, Equation 7), and the threshold for a confident detection may reasonably be taken to be ten times this value. Parameters for this experiment are also listed in Table 2. Note that the integration period of the Juno MWR is too long for it to detect a ns-scale pulse from a Jovian air shower, and the orbit of this probe is also unsuitable; this experiment represents the potential sensitivity of a similar instrument optimised for this application.

Calculating the cosmic-ray aperture of these experiments with Equation 8, we find their projected differential limits on the cosmic-ray flux as

$$\frac{dF}{dE} < \frac{2.3}{EA(E)t_{\rm obs}} \qquad (9)$$

where $t_{\rm obs}$ is the total observing time and the factor of 2.3 comes from the Poissonian distribution of the expected number of events for a 90%-confidence limit. These projected limits, shown in Figure 8, are well above the energy of the known cosmic-ray flux. Their energy range is suitable for testing predicted cosmic-ray fluxes from exotic top-down mechanisms, such as the decay of superheavy dark matter (Aloisio et al. 2015); models of this class are generally constrained by limits on the fluxes of ultra-high-energy neutrinos (Gorham et al. 2010) and photons (Abraham et al. 2009), but not entirely ruled out. However, even these speculative fluxes are too low to be detected by these experiments by over three orders of magnitude.

6. Discussion

The prospect of utilising Jupiter with its 6×10^{10} km^2 of surface area as a cosmic-ray detector is an attractive one. The only larger body in the solar system, the Sun, is a strong source of background radiation that makes it highly impractical to use in this role. Consequently, no larger cosmic-ray aperture than that of Jupiter will be available for the foreseeable future.

TABLE 2
POTENTIAL SENSITIVITY OF COHERENT PULSE DETECTION EXPERIMENTS

Experiment	Threshold ($\mathcal{E}_{\rm thr}/(\mu$V/m/MHz))	Frequency (ν/MHz)	Distance (l/m)	Observing time ($t_{\rm obs}$/h)
LUNASKA Parkes	0.0047	1350	8×10^{11}	127.2
SKA-lunar	0.0014	225	8×10^{11}	1000
Juno MWR	2.9	600	2×10^{8}[a]	8760[b]

[a]Minimum distance at which Jupiter fits within the antenna beam.

[b]Total nominal Jupiter-orbiting operation of the Juno mission.

NOTE.—None of these experiments are/were designed to detect Jovian air showers. These parameters reflect their potential sensitivity if they had been so designed.

References. — (Bray et al. 2015a,b; Janssen et al. 2014)

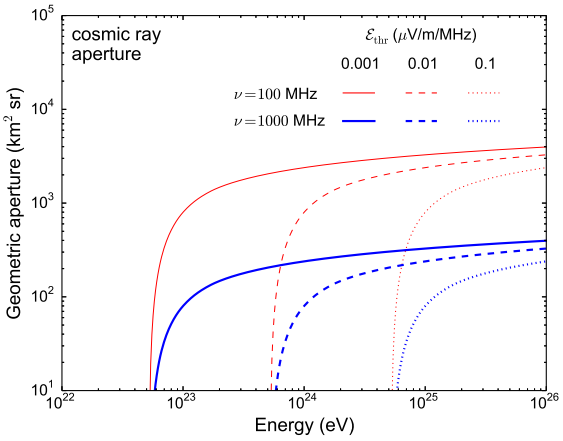

Fig. 7.— Geometric apertures of Earth-based radio antennas for the detection of cosmic rays interacting in the atmosphere of Jupiter. The minimum detectable cosmic-ray energy is determined by the radio detection threshold $\mathcal{E}_{\rm thr}$, and the maximum geometric aperture is determined by the observing frequency ν.

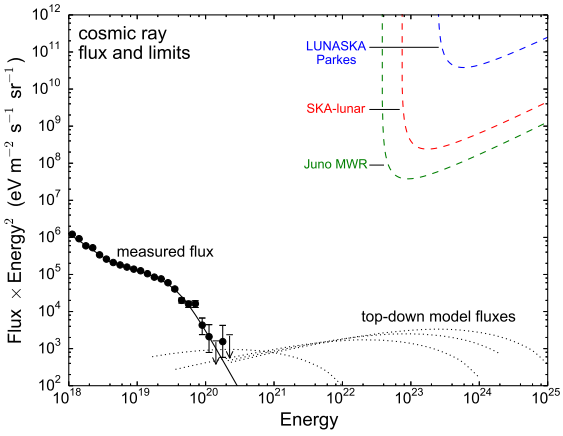

Fig. 8.— Ultra-high-energy cosmic-ray flux and potential limits from radio observations of Jupiter. The points and solid line show the measured cosmic-ray flux and fit (Abraham et al. 2010), while dotted lines show speculative cosmic-ray proton fluxes from decay of super-heavy dark matter (Aloisio et al. 2015). Dashed lines show potential limits from radio searches for Jovian air showers with the experiments described in the text.

However, searches for radio emission from Jovian air showers are not a practical means of exploiting Jupiter as a cosmic-ray detector. We have found in this work that, with present or near-future instruments, this technique is sensitive only to cosmic rays above an extremely high threshold, $\sim 10^{23}$ eV. Furthermore, we have also found that it is sensitive only to extremely high cosmic-ray fluxes, more than three orders of magnitude higher than the most optimistic predicted fluxes in this energy range. Our results here are not precise — we have, for example, inaccuracy of a factor ~ 2 in our parameterisation of the radio emission from a shower — but a more precise analysis is unlikely to be so much more optimistic than this work that it predicts this technique to be practical.

The major effect identified in this work is that, for the forward-beamed radio emission from a shower to escape Jupiter, the shower must be inclined almost horizontally, which causes it to develop in the upper atmosphere where the density is low. In this environment, the radio emission is very narrowly beamed, which leads to a small cosmic-ray acceptance angle and hence a small geometric aperture. It is possible for forward-beamed radio emission to escape from a shower deeper in the atmosphere if the shower is directed upwards, which may occur if the shower is initiated by a neutrino that has passed through a substantial fraction of Jupiter, but the large neutrino-nucleon cross-section at ultra-high energies will constrain neutrinos to trajectories that follow a shallow chord through the planet, as it does in the case of the Moon (Jaeger et al. 2010, Figure 1). We therefore expect the geometric aperture of this technique for neutrinos to be similarly small.

We expect similar results to apply for the other gas giant planets in our solar system. Each of them has a smaller radius than does Jupiter, which allows a horizontally-inclined shower to develop at a lower altitude, but each also has a lower surface gravity and hence a larger atmospheric scale height, so the density at a given altitude will be reduced; combined, these effects may cause the typical density under which an air shower develops and hence its radio emission to increase or decrease slightly. The magnetic fields of the other gas giants are also weaker than that of Jupiter (e.g. Saturn, 21 μT; Davis & Smith 1990), which will reduce the strength of radio emission from showers in their atmospheres, though it will also ameliorate the shower suppression due to synchrotron losses. Finally, all of the other gas giants are more distant than Jupiter, reducing the effectiveness of Earth-based instruments.

Our results also apply to other forms of radiation emitted by a Jovian air shower, provided that they are beamed at the Cherenkov angle and do not penetrate the lower atmosphere of Jupiter more efficiently than radio. Optical Cherenkov radiation meets these conditions, and so is also excluded as a practical means of detecting Jovian air showers.

Our results do not exclude the possibility of practical detection of Jovian air showers through an emission mechanism that radiates isotropically, such as atmospheric fluorescence. Orbital detection of atmospheric fluorescence from terrestrial air showers in the 330–400 nm band is being pursued by the JEM-EUSO project (Takahashi 2009), and the same technique could be applied with an imaging telescope in orbit around Jupiter. The depth at which an air shower can be detected will be limited by Rayleigh scattering, for which an optical depth of unity for the JEM-EUSO band is reached in the Jovian atmosphere at a pressure of ~ 2000 mbar (West et al. 2004, Figure 5.3), slightly deeper than the minimum altitude for radio detection found in this work. However, the JEM-EUSO band is tuned to the fluorescence spectrum of nitrogen, which is almost non-existent in the Jovian atmosphere. Molecular hydrogen fluoresces primarily at wavelengths < 200 nm (Sternberg 1989), which are much more strongly affected by Rayleigh scattering; better results may be obtained with the helium line at 502 nm (Becker et al. 2010). The application of this technique to Jupiter seems to offer no compelling advantages, but may become worthwhile at some point in the future if the aperture provided by the Earth is fully exploited.

The authors would like to thank Jaime Alvarez-Muñiz and Washington Carvalho Jr. for helpful discussions concerning ZHAireS. JDB acknowledges support from ERC-StG 307215 (LODESTONE). AN is supported by the DFG (research fellowship NE 2031/1-1).

REFERENCES

Aab, A., Abreu, P., Aglietta, M., et al. 2014, Phys. Rev. D, 90, 122006

—. 2015, Nucl. Instrum. Meth. A, 798, 172

Abraham, J., Abreu, P., Aglietta, M., et al. 2009, Astropart. Phys., 31, 399

—. 2010, Phys. Lett. B, 685, 239

Allan, H. R. 1971, in Progress in Elementary Particle and Cosmic Ray Physics, Vol. 10, Progress in Elementary Particle and Cosmic Ray Physics, ed. J. G. Wilson & S. A. Wouthuysen (Amsterdam/London: North-Holland), 171–302

Aloisio, R., Matarrese, S., & Olinto, A. V. 2015, J. Cosmology Astropart. Phys., 8, 24

Alvarez-Muñiz, J., Carvalho, W. R., Tueros, M., & Zas, E. 2012, Astropart. Phys., 35, 287

Alvarez-Muñiz, J., Marqués, E., Vázquez, R. A., & Zas, E. 2006, Phys. Rev. D, 74, 023007

Becker, F., Forck, P., Giacomini, T., Haseitl, R., & Walasek-Hoehne, B. 2010, in Proc. 14th Beam Instrumentation Workshop, Joint Accelerator Conferences Website, 156–159

Bray, J. 2016, Astropart. Phys., 77, 1

Bray, J. D., Ekers, R. D., Roberts, P., et al. 2015a, Astropart. Phys., 65, 22

Bray, J. D., Alvarez-Muñiz, J., Buitink, S., et al. 2015b, in Proc. Sci., Vol. 215, Advancing Astrophysics with the Square Kilometre Array, 144

Buitink, S., Corstanje, A., Falcke, H., et al. 2016, Nature, 531, 70

Davis, Jr., L., & Smith, E. J. 1990, J. Geophys. Res., 95, 15257

Finlay, C. C., Maus, S., Beggan, C. D., et al. 2010, Geophys. J. Int'l, 183, 1216

Gorham, P. W. 2004, Planet-sized Detectors for Ultra-high Energy Neutrinos & Cosmic Rays, Capability roadmap, NASA Advanced Planning Office, arXiv:astro-ph/0411510

Gorham, P. W., Allison, P., Baughman, B. M., et al. 2010, Phys. Rev. D, 82, 022004

Henriksen, T., & Baarli, J. 1957, Radiation Res., 6, 415

Huege, T. 2016, ArXiv e-prints, arXiv:1601.07426

Jaeger, T. R., Mutel, R. L., & Gayley, K. G. 2010, Astropart. Phys., 34, 293

Janssen, M. A. 2015, priv. comm.

Janssen, M. A., Brown, S. T., Oswald, J. E., & Kitiyakara, A. 2014, in Proc. IRMMW-THz 2014

Kahn, F. D., & Lerche, I. 1966, Proc. R. Soc. A, 289, 206

Lindal, G. F., Wood, G. E., Levy, G. S., et al. 1981, J. Geophys. Res., 86, 8721

Moses, J. I., Fouchet, T., Bézard, B., et al. 2005, J. Geophys. Res., 110, 8001

Nelles, A., Buitink, S., Falcke, H., et al. 2015, Astropart. Phys., 60, 13

Olive, K. A., Agashe, K., Amsler, C., et al. 2014, Chinese Phys. C, 38, 090001

Privitera, P., & Motloch, P. 2014, ApJ, 791, L15

Rimmer, P. B., Stark, C. R., & Helling, C. 2014, ApJ, 787, L25

Sciutto, S. J. 1999, AIRES: A system for air shower simulations, Tech. rep., Pierre Auger Collaboration, arXiv:astro-ph/9911331

Smith, E. J., Davis, Jr., L., Jones, D. E., et al. 1974, J. Geophys. Res., 79, 3501

Sternberg, A. 1989, ApJ, 347, 863

Takahashi, Y. 2009, New J. Phys., 11, 065009

Tueros, M., & Sciutto, S. 2010, Comput. Phys. Commun., 181, 380

Warwick, J. W. 1967, Space Sci. Rev., 6, 841

West, R. A., Baines, K. H., Friedson, A. J., et al. 2004, in Jupiter: The Planet, Satellites and Magnetosphere, ed. F. Bagenal, T. E. Dowling, & W. B. McKinnon (Cambridge University Press), 79–104

This 2-column preprint was prepared with the AAS LaTeX

macros v5.2.